

ARTICLE

Suzuki–Miyaura Cross-Coupling of Esters by Selective O–C(O) Cleavage Mediated by Air- and Moisture-Stable $[\text{Pd}(\text{NHC})(\mu\text{-Cl})\text{Cl}]_2$ Precatalysts: Catalyst Evaluation and Mechanism

Received 00th January 20xx,
Accepted 00th January 20xx

DOI: 10.1039/x0xx00000x

The cross-coupling of aryl esters has emerged as a powerful platform for the functionalization of otherwise inert acyl C–O bonds in chemical synthesis and catalysis. Herein, we report a combined experimental and computational study on the acyl Suzuki–Miyaura cross-coupling of aryl esters mediated by well-defined, air- and moisture-stable Pd(II)–NHC precatalysts $[\text{Pd}(\text{NHC})(\mu\text{-Cl})\text{Cl}]_2$. We present a comprehensive evaluation of $[\text{Pd}(\text{NHC})(\mu\text{-Cl})\text{Cl}]_2$ precatalysts and compare them with the present state-of-the-art $[(\text{Pd}(\text{NHC})\text{allyl})]$ precatalysts bearing allyl-type throw-away ligands. Most importantly, the study reveals $[\text{Pd}(\text{NHC})(\mu\text{-Cl})\text{Cl}]_2$ as the most reactive precatalysts discovered to date in this reactivity manifold. The unique synthetic utility of this unconventional O–C(O) cross-coupling is highlighted in the late-stage functionalization of pharmaceuticals and sequential chemoselective cross-coupling, providing access to valuable ketone products by a catalytic mechanism involving Pd insertion into the aryl ester bond. Furthermore, we present a comprehensive study of the catalytic cycle by DFT methods. Considering the clear advantages of $[\text{Pd}(\text{NHC})(\mu\text{-Cl})\text{Cl}]_2$ precatalysts on several levels, including facile one-pot synthesis, superior atom-economic profile to all other Pd(II)–NHC catalysts, and versatile reactivity, these should be considered as the ‘first-choice’ catalysts for all routine applications in ester O–C(O) bond activation.

Introduction

Transition-metal-catalyzed cross-coupling reactions are of tremendous importance in organic synthesis and catalysis.^{1,2} In this context, the cross-coupling platform utilizing classical C–X electrophiles provides arguably the most convenient access to a broad variety of structural motifs across numerous facets of chemistry, biology and materials science as highlighted by the 2010 Nobel Prize in Chemistry.^{3,4}

In recent years, particular advances have been made in the development of unconventional cross-coupling electrophiles that are normally problematic due to slow oxidative addition to a metal catalyst.^{5,6} In this respect, the progress achieved in the C–N, C–O and C–S activation/cross-coupling of C(sp²)–X electrophiles is noteworthy.^{7–10} On the other hand, recent impetus has been gained by the discovery of C(acyl)–X cross-coupling of bench-stable acyl electrophiles that enable the direct modification of amides¹¹ and esters¹² by a catalytic

mechanism involving versatile acyl-metal intermediates (Fig. 1). In the vast majority, the enhancement of catalytic activity has been achieved by judicious ligand design, wherein the ancillary ligand facilitates elementary steps in the catalytic cycle, including oxidative addition and reductive elimination.^{13,14} To further exploit the full potential of cross-coupling reactions,¹⁵ it is imperative that new, more active catalysts systems be identified and that the underlying mechanistic aspects of the high catalytic activity be clearly elucidated.

In this context, we have identified air-stable NHC–Pd(II) chloro dimers, $[\text{Pd}(\text{NHC})(\mu\text{-Cl})\text{Cl}]_2$, as the preferred Pd(II)–NHC catalysts for C(sp²)–Cl and C(acyl)–N cross-coupling.^{15–17} While performing further reactions using these catalysts, we probed the Suzuki–Miyaura cross-coupling of aryl esters. Herein, we present a combined experimental and computational study of the Suzuki–Miyaura coupling of aryl esters by a highly selective O–C(O) cleavage using well-defined, air- and moisture-stable $[\text{Pd}(\text{NHC})(\mu\text{-Cl})\text{Cl}]_2$ precatalysts. Acyl O–C(O) cleavage of aryl esters is significantly more challenging than N–C(O) cleavage of amides. At present, there are no phosphine-based systems for this reaction, which highlights the challenge of bond activation and the beneficial use of strongly σ -donating NHC ligands.

Most crucially, this study reveals $[\text{Pd}(\text{NHC})(\mu\text{-Cl})\text{Cl}]_2$ as the most reactive precatalysts discovered to date in this reactivity manifold. A comprehensive study of the catalytic cycle by DFT methods reveals that the great advantage of these $[\text{Pd}(\text{NHC})(\mu\text{-Cl})\text{Cl}]_2$ precatalysts is the much easier activation to yield the

^a Department of Chemistry, Rutgers University, 73 Warren Street, Newark, NJ 07102, United States. E-mail: michal.szostak@rutgers.edu.

^b Institut de Química Computacional i Catàlisi and Departament de Química, Universitat de Girona, Campus Montilivi, 17003 Girona, Catalonia, Spain. E-mail: albert.poater@udg.edu

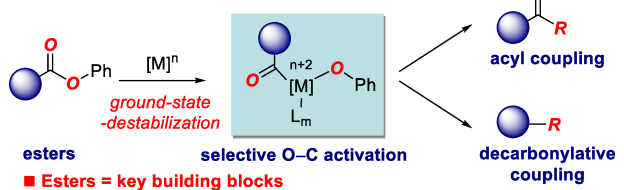
^c King Abdullah University of Science & Technology, KAUST Catalysis Center (KCC), 23955-6900 Thuwal, Saudi Arabia.

^d Department of Chemistry, Ghent University, Krijgslaan 281, S-3, B-9000 Ghent, Belgium. E-mail: steven.nolan@ugent.be

Electronic Supplementary Information (ESI) available: Experimental details and computational data. See DOI: 10.1039/x0xx00000x

mono-ligated $\text{Pd}(0)\text{-NHC}$ than with allyl $\text{Pd}\text{-NHC}$ precatalysts. The unique synthetic utility is highlighted in the late-stage functionalization of pharmaceuticals and sequential chemoselective coupling. Considering the clear advantages of $[\text{Pd}(\text{NHC})(\mu\text{-Cl})\text{Cl}]_2$ precatalysts on several levels, such as facile one-pot synthesis, much superior atom-economic profile to all other $\text{Pd}(\text{II})\text{-NHC}$ catalysts, and versatile reactivity, these (pre)-catalysts should be considered as the ‘first-choice’ catalysts for all routine applications in ester $\text{O}\text{-C(O)}$ bond activation.

A: Ester bond C–O cross-coupling: new platform for catalysis



B: Acyl Suzuki–Miyaura cross-coupling of esters: new catalytic platform

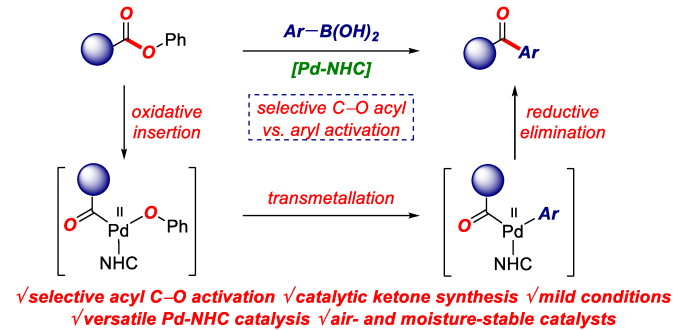


Fig. 1 (a) Cross-coupling of esters by $\text{O}\text{-C(O)}$ activation; (b) Acyl Suzuki–Miyaura cross-coupling of aryl esters.

Results and Discussion

Catalyst Evaluation. We initiated our study by evaluating the reaction conditions using $[\text{Pd}(\text{IPr})(\mu\text{-Cl})\text{Cl}]_2$ catalyst **1** on a model system (Table 1, Fig. 2).^{17,18} Importantly, catalyst **1** is commercially available, while its synthesis proceeds in a single, high-yielding step from $\text{IPr}\text{-HCl}$, $\text{Pd}(\text{OAc})_2$ and K_2CO_3 , followed by the addition of HCl (Chart 1),^{15–17} making it easily and readily available for small and large scale catalytic investigations. As shown, the desired $\text{O}\text{-C(O)}$ cross-coupling occurred under exceedingly mild room temperature conditions in the presence of $[\text{Pd}(\text{IPr})(\mu\text{-Cl})\text{Cl}]_2$ (**1**) (0.25 mol%) and K_2CO_3 as a mild carbonate base in THF (Table 1, entry 1). Several other solvents (entries 2–6) and bases (entries 7–13) were examined, however, the cross-coupling was less efficient under these conditions. The addition of water is important as the reaction was almost completely suppressed in the absence of water under these conditions (entry 14).^{18a} Finally, a TON of 670 was determined for the cross-coupling at 40 °C (entry 15), consistent with the high reactivity of this catalyst system (*vide infra*).

Next, we focused on evaluating the performance of the $[\text{Pd}(\text{IPr})(\mu\text{-Cl})\text{Cl}]_2$ catalyst vs. other halo dimer catalysts and $[\text{Pd}(\text{NHC})(\text{allyl})\text{Cl}]$ type catalysts bearing allyl-type throw-away ligand.^{11a,17} The structures of well-defined $\text{Pd}(\text{II})\text{-NHC}$ catalysts selected for this study are presented in Fig. 2.

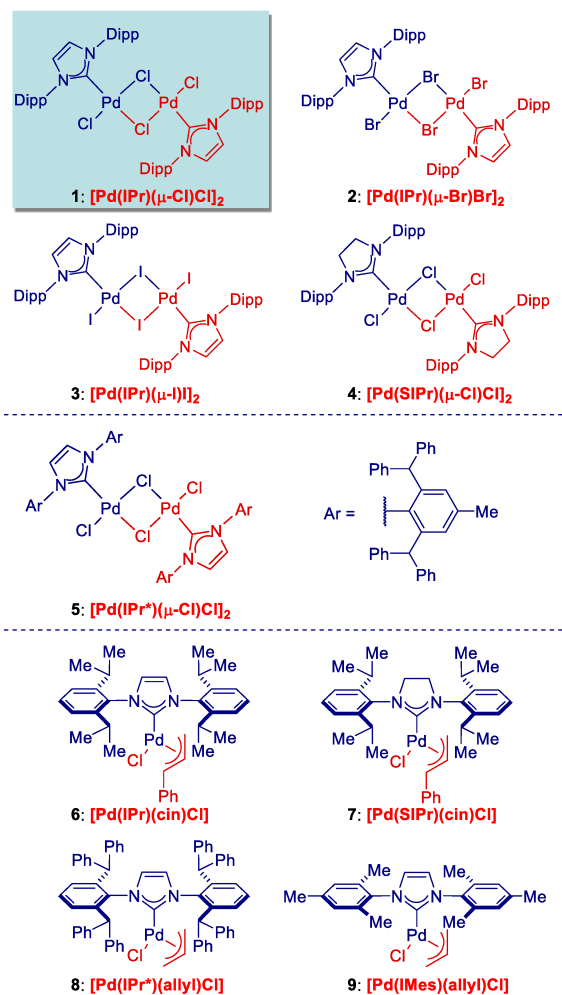


Fig. 2 Structures of $\text{Pd}(\text{II})\text{-NHC}$ catalysts **1–9** used in this study (Dipp = 2,6-*i*Pr₂-C₆H₃).

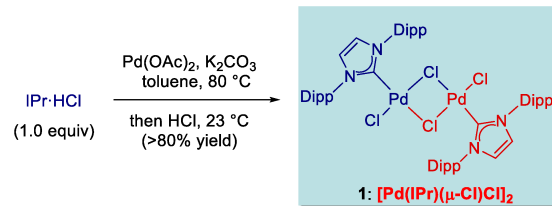
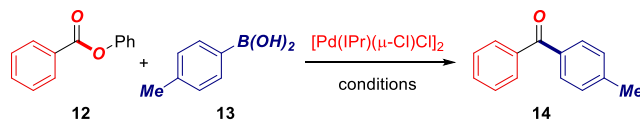


Chart 1 Facile, one-pot synthesis of $[\text{Pd}(\text{NHC})(\mu\text{-Cl})\text{Cl}]_2$ precatalysts.

First, evaluation of the bromo- and iodo-based dimers, revealed that $[\text{Pd}(\text{IPr})(\mu\text{-Br})\text{Br}]_2$ (**2**) and $[\text{Pd}(\text{IPr})(\mu\text{-I})\text{I}]_2$ (**3**) catalysts are less reactive than the chloro congener $[\text{Pd}(\text{IPr})(\mu\text{-Cl})\text{Cl}]_2$ (**1**) (Table 2, entries 1–6). In case of the bromo dimer catalyst, $[\text{Pd}(\text{IPr})(\mu\text{-Br})\text{Br}]_2$ (**2**), the cross-coupling occurred at 60 °C, while no reaction was observed at 23 °C, while the iodo dimer, $[\text{Pd}(\text{IPr})(\mu\text{-I})\text{I}]_2$ (**3**), was ineffective at 60 °C, yet the cross-coupling occurred at 80 °C. These experiments indicate the following order of reactivity of the dimer catalysts in the $\text{O}\text{-C(O)}$ cross-coupling: Cl > Br > I, which is closely related to the rate of activation to yield the mono-ligated $\text{Pd}(0)\text{-NHC}$ species (*vide infra*).¹⁹ Next, it was of considerable interest to evaluate the performance of the imidazolylidene-based chloro dimer catalyst $[\text{Pd}(\text{IPr})(\mu\text{-Cl})\text{Cl}]_2$ (**1**) with its imidazolinylidene analogue

Table 1 Optimization of Reaction Conditions^a

entry	base	solvent	T (°C)	yield (%)
1	K ₂ CO ₃	THF	23	>95
2	K ₂ CO ₃	toluene	23	<5
3	K ₂ CO ₃	dioxane	23	<2
4	K ₂ CO ₃	DME	23	75
5	K ₂ CO ₃	CH ₃ CN	23	<2
6	K ₂ CO ₃	EtOH	23	27
7	Li ₂ CO ₃	THF	23	<2
8	Na ₂ CO ₃	THF	23	34
9	Cs ₂ CO ₃	THF	23	52
10	CsF	THF	23	57
11	KF	THF	23	70
12	K ₃ PO ₄	THF	23	<2
13	KOH	THF	23	5
14 ^b	K ₂ CO ₃	THF	23	13
15 ^c	K ₂ CO ₃	THF	40	67

^aConditions: ester (1.0 equiv), 4-Tol-B(OH)₂ (2.0 equiv), [Pd(IPr)(μ-Cl)Cl]₂ (0.25 mol%), K₂CO₃ (3.0 equiv), H₂O (5 equiv), solvent (0.25 M), T, 12 h. ^bw/o water. ^c[Pd(IPr)(μ-Cl)Cl]₂ (0.05 mol%), THF (0.5 M). See ESI for details.

[Pd(SIPr)(μ-Cl)Cl]₂ (4) (SIPr = 1,3-bis(2,6-diisopropylphenyl)imidazolidin-2-ylidene) and the sterically-bulky imidazolylidene [Pd(IPr*)(μ-Cl)Cl]₂ (5) (IPr* = 1,3-bis(2,6-bis(diphenylmethyl)-4-methylphenyl)imidazol-2-ylidene)²⁰ (Table 2, entries 7-9). Interestingly, the following order of reactivity was established: [Pd(IPr)(μ-Cl)Cl]₂ (1) > [Pd(SIPr)(μ-Cl)Cl]₂ (4) > [Pd(IPr*)(μ-Cl)Cl]₂ (5), while the latter catalyst was unproductive at 23 °C, consistent with its slower activation to give the mono-ligated Pd(0)-NHC (*vide infra*).

Next, we were interested in evaluating the performance of [Pd(NHC)(allyl)Cl] type catalysts. These catalysts, introduced by one of us (S.P.N.) in 2002,¹⁷ are among the most popular, commercially-available Pd(II)-NHC catalysts for a broad variety of cross-coupling applications used worldwide. Remarkably, we found that the chloro dimer catalyst [Pd(IPr)(μ-Cl)Cl]₂ (1) is more reactive in the O-C(O) cross-coupling than the cinnamyl-based [Pd(IPr)(cin)Cl] (6) and [Pd(SIPr)(cin)Cl] (7) as well as allyl-based [Pd(IPr*)(allyl)Cl] (8) and [Pd(IMes)(allyl)Cl] (9), demonstrating the superior reactivity of the chloro dimer under these conditions. To further probe the high reactivity of [Pd(IPr)(μ-Cl)Cl]₂ (1), we performed kinetic profiling studies using [Pd(IPr)(μ-Cl)Cl]₂ (1) as well as allyl-based congeners [Pd(IPr)(cin)Cl] (6) and [Pd(IPr)(t-Bu-ind)Cl] (10)^{14b,d} and the heterocycle-based Pd-PEPPSI-IPr (11)^{14c,15e} (Fig. 3). Kinetic profiling studies revealed that [Pd(IPr)(μ-Cl)Cl]₂ (1) (red squares) is superior to [Pd(IPr)(cin)Cl] (6), Pd-PEPPSI-IPr (11) (green squares) and [Pd(IPr)(t-Bu-ind)Cl] (10) (yellow squares) with the latter showing the poorest performance under these conditions. The high reactivity of the chloro dimer catalyst [Pd(IPr)(μ-Cl)Cl]₂ (1) is consistent with facile catalyst activation by dimer dissociation. Note that the kinetic profile for the formation of 14 is identical ($\pm 2\%$) to the conversion of 12.

Table 2 Comparison of Reactivity of Pd(II)-NHC Precatalysts 1-9^a

entry	[Pd-NHC]	T (°C)	yield (%)
1	[Pd(IPr)(μ-Cl)Cl] ₂ (1)	23	>95
2	[Pd(IPr)(μ-Br)Br] ₂ (2)	23	<2
3	[Pd(IPr)(μ-I)] ₂ (3)	23	<2
4	[Pd(IPr)(μ-Br)Br] ₂ (2)	60	59
5	[Pd(IPr)(μ-I)] ₂ (3)	60	<2
6	[Pd(IPr)(μ-I)] ₂ (3)	80	46
7	[Pd(SIPr)(μ-Cl)Cl] ₂ (4)	23	76
8	[Pd(IPr*)(μ-Cl)Cl] ₂ (5)	23	<2
9	[Pd(IPr*)(μ-Cl)Cl] ₂ (5)	60	67
10	[Pd(IPr)(cin)Cl] (6)	23	66
11	[Pd(SIPr)(cin)Cl] (7)	23	64
12	[Pd(IPr*)(allyl)Cl] (8)	23	<2
13	[Pd(IMes)(allyl)Cl] (9)	23	<2

^aConditions: ester (1.0 equiv), 4-Tol-B(OH)₂ (2.0 equiv), [Pd] (0.50 mol%), K₂CO₃ (3.0 equiv), H₂O (5 equiv), THF (0.25 M), T, 12 h. See ESI for details.

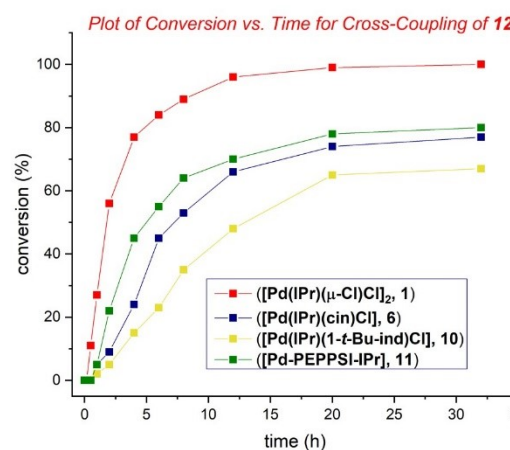
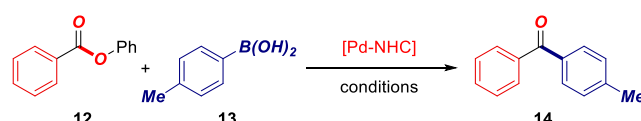
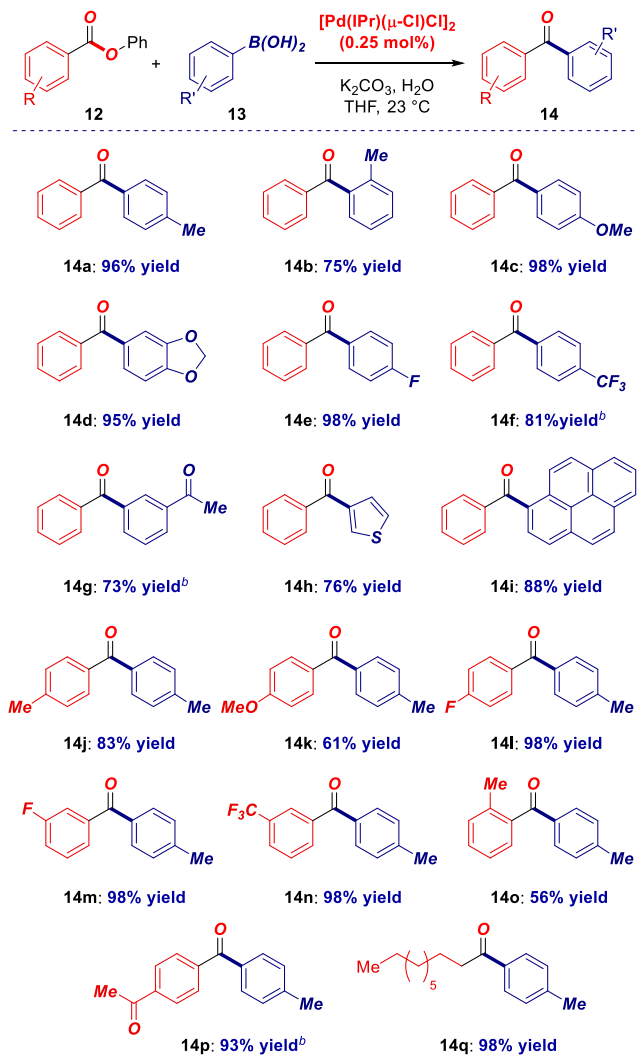


Fig. 3 Kinetic profile in the acyl Suzuki-Miyaura cross-coupling with 4-Tol-B(OH)₂. Conditions: ester (1.0 equiv), 4-Tol-B(OH)₂ (2.0 equiv), [Pd] (0.5 mol%), K₂CO₃ (3.0 equiv), H₂O (5 equiv), THF (0.25 M), 23 °C, 0-32 h. [Pd] = [Pd(IPr)(μ-Cl)Cl]₂ (1); [Pd(IPr)(cin)Cl] (6); [Pd(IPr)(t-Bu-ind)Cl] (10); [Pd-PEPPSI-IPr] (11).

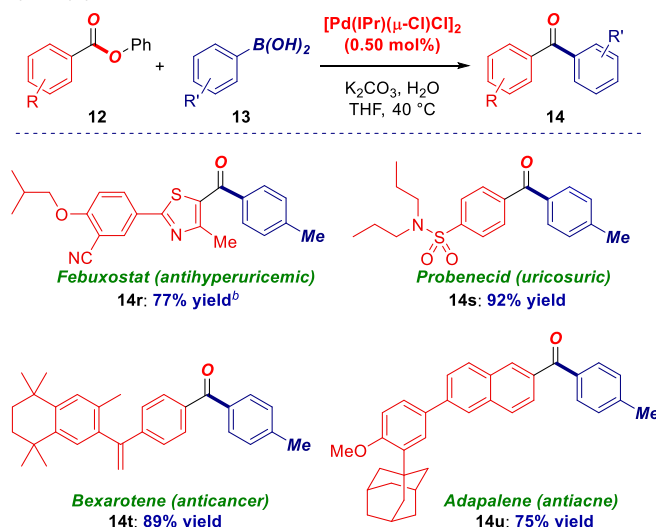
Substrate Scope. Having identified [Pd(IPr)(μ-Cl)Cl]₂ (1) as the preferred catalyst for the O-C(O) cross-coupling, we probed the versatility of this catalyst on the Suzuki-Miyaura cross-coupling of aryl esters (Table 3). As shown in Table 3, this catalyst is amenable to effect the cross-coupling of a broad range of aryl esters and boronic acids, including neutral (14a), sterically-hindered (14b), electron-rich (14c-14d), electron-deficient (14e-14g), heterocyclic (14h) and polyaromatic (14i)

Table 3 Scope of the Suzuki–Miyaura Cross-Coupling of Aryl Esters using Chloro Dimer $[\text{Pd}(\text{IPr})(\mu\text{-Cl})\text{Cl}]_2$ (1)^a

^aConditions: ester (1.0 equiv), Ar-B(OH)₂ (2.0 equiv), $[\text{Pd}(\text{IPr})(\mu\text{-Cl})\text{Cl}]_2$ (0.25 mol%), K_2CO_3 (3.0 equiv), H_2O (5 equiv), THF (0.25 M), 23 °C, 12 h. ^b $[\text{Pd}(\text{IPr})(\mu\text{-Cl})\text{Cl}]_2$ (0.50 mol%), 60 °C.

boronic acids as well as electron-rich (**14j–14k**), electron-poor (**14l–14o**), sterically-hindered (**14p**) and aliphatic aryl esters (**14q**). The functional group tolerance to electrophilic functionalities, such as ketones (**14g**, **14o**) and full selectivity for the O–C(O) acyl cleavage under mild conditions are particularly noteworthy features of this catalyst.

Late-Stage Functionalization. In consideration of the tremendous utility of cross-coupling reactions in the late-stage functionalization of pharmaceuticals,²¹ we explored the acyl cross-coupling of aryl esters derived from APIs using $[\text{Pd}(\text{IPr})(\mu\text{-Cl})\text{Cl}]_2$ (1) (Table 4). As shown, the cross-coupling of aryl esters of *Febuxostat* (antihyperuricemic) (**14r**), *Probenecid* (uricosuric) (**14s**), *Bexarotene* (anticancer) (**14t**) and *Adapalene* (antiacne) (**14u**) proceeded in excellent yields, further demonstrating the functional group tolerance and potential impact of the catalyst on the synthesis of biologically active products.

Table 4 Late-Stage Functionalization of Pharmaceuticals by Suzuki–Miyaura Cross-Coupling of Aryl Esters using Chloro Dimer $[\text{Pd}(\text{IPr})(\mu\text{-Cl})\text{Cl}]_2$ (1)^a

^aConditions: ester (1.0 equiv), Ar-B(OH)₂ (2.0 equiv), $[\text{Pd}(\text{IPr})(\mu\text{-Cl})\text{Cl}]_2$ (0.50 mol%), K_2CO_3 (3.0 equiv), H_2O (5 equiv), THF (0.25 M), 40 °C, 12 h. ^b $[\text{Pd}(\text{IPr})(\mu\text{-Cl})\text{Cl}]_2$ (1.0 mol%), 60 °C.

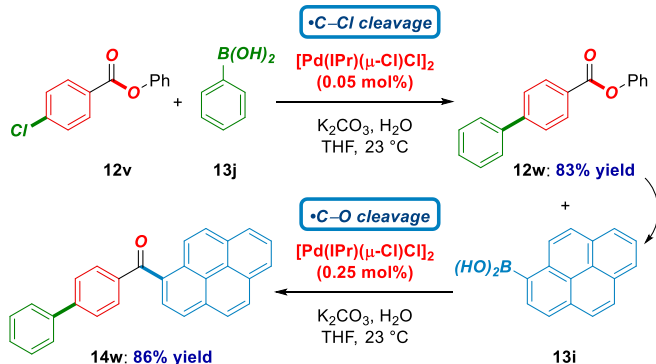
Selectivity Studies. Considering the unique versatility of $[\text{Pd}(\text{IPr})(\mu\text{-Cl})\text{Cl}]_2$ (1), we probed its application to the orthogonal sequential C(sp²)–Cl/C(acyl)–O cross-couplings (Scheme 1).^{1–3} As shown, the Suzuki–Miyaura cross-coupling of phenyl 4-chlorobenzoate proceeded chemoselectively at the C(sp²) carbon, followed by the C(acyl)–O activation to give the extensively conjugated biaryl ketone (**14w**). This class of π-conjugated ketones serves as precursors in materials science,²² while the reaction established the following order of reactivity: C–Cl > O–C(O), consistent with the challenging oxidative addition of the ester bond.

Furthermore, we were interested to probe the selectivity of ester O–C(O) activation vs. amide N–C(O) activation by $[\text{Pd}(\text{IPr})(\mu\text{-Cl})\text{Cl}]_2$ (1) (Scheme 2). Amide bond activation has recently emerged as an enabling platform for the cross-coupling of classical amide bonds.¹¹ In these experiments, we observed complete selectivity for the N–C(O) cross-coupling vs. O–C(O) cross-coupling (N-Boc/Me vs. OPh, N-Boc/Ph vs. OPh), consistent with the isomerization barrier around the X–C(O) (X = N, O) bond.²³ Thus, aryl esters should be considered as more stable acyl equivalents than N-Boc activated amide bonds.

A major direction in the development of Pd(II)–NHC catalytic systems involves eco-friendly solvents and reaction conditions for the application of Pd–NHC catalysts.²⁴ We were pleased to find that sustainable, eco-derived 2-MeTHF as well as benign EtOAc could be used as solvents to yield the ketone product in excellent yields using $[\text{Pd}(\text{IPr})(\mu\text{-Cl})\text{Cl}]_2$ (1) as catalyst (Scheme 3). The full selectivity for the cross-coupling of an aryl O–C(O) bond (–OPh) in the presence of alkyl O–C(O) bond in EtOAc solvent is noteworthy and demonstrates the synthetic possibilities by activation of unconventional electrophiles.

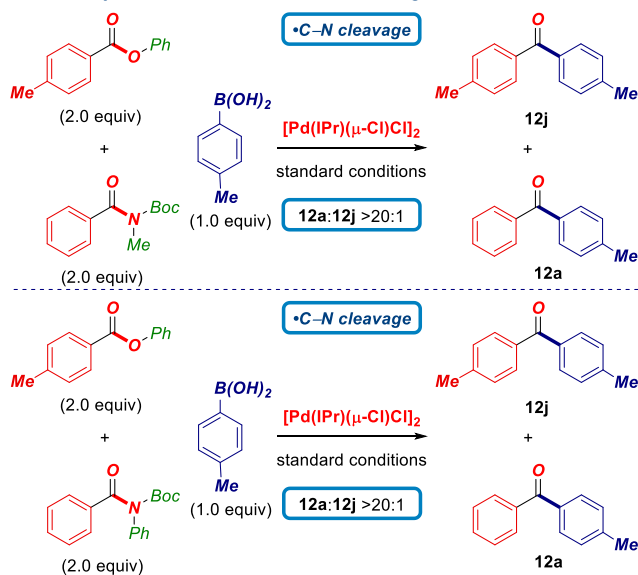
Scheme 1 Sequential Orthogonal C–Cl/C–O Cross-Coupling using Chloro Dimer $[\text{Pd}(\text{IPr})(\mu\text{-Cl})\text{Cl}]_2$ (1)

■ **Chemoselective Sequential Cross-Coupling: C–Cl > C–O**

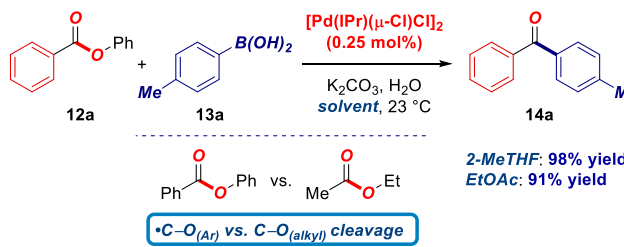


Scheme 2 Selectivity of C–N vs. C–O Cross-Coupling using Chloro Dimer $[\text{Pd}(\text{IPr})(\mu\text{-Cl})\text{Cl}]_2$ (1)

■ **Selectivity of Amide C–N vs. Ester C–O Cleavage**



Scheme 3 Suzuki–Miyaura Cross-Coupling of Aryl Esters using Chloro Dimer $[\text{Pd}(\text{IPr})(\mu\text{-Cl})\text{Cl}]_2$ (1) in Eco-Friendly Solvents



Finally, it is worth noting TON (TON = turnover number) of 3,000 obtained using the chloro dimer catalyst $[\text{Pd}(\text{IPr})(\mu\text{-Cl})\text{Cl}]_2$ (1) at 0.0125 mol% loading at 80 °C (4-Tol-B(OH)₂ (2 equiv), K₂CO₃ (3 equiv), THF, not shown). This finding further supports the excellent reactivity of this class of chloro-bridged dimer catalysts and bodes well for future application in selective O–C(O) cleavage.

Computational Studies. To shed light on the mechanism density functional theory (DFT) calculations (M06/Def2-TZVP~sdd(PCM-THF)/BP86-D3/SVP~sdd) of the cross-coupling reaction using the phenyl ester and Ph-B(OH)₂ reagents were carried out (see Fig. 4). From the catalytic active species Pd(0) the coordination of the phenyl ester leads to the C–O bond cleavage that leaves the phenoxide moiety on the metal, overcoming an energy barrier of 12.6 kcal/mol for this oxidative addition. The subsequent intermediate is stabilized 11.6 kcal/mol by the coordination of the base, *i.e.* K₂CO₃, that assists in the phenoxide ligand dissociation from the metal assisted by a potassium counteraction, with a kinetic cost of 12.3 kcal/mol. The second reagent then enters the scene for the transmetalation, not coordinating directly to the metal, but to one of the oxygen atoms from the old base, *i.e.* the Ph-B(OH)₂ bonds to the ionic KCO₃ moiety. Boron transfers its phenyl to the metal, at a kinetic cost of 20.7 kcal/mol. And thermodynamically, the process is also very favorable once the K₂CO₃(B(OH)₂OPh) fragment dissociates, specifically 10.8 kcal/mol. The reductive elimination is then very easy from both the kinetic (2.7 kcal/mol) and thermodynamic (26.0 kcal/mol) point of view, closing the cycle, which is exoergic by 29.2 kcal/mol.

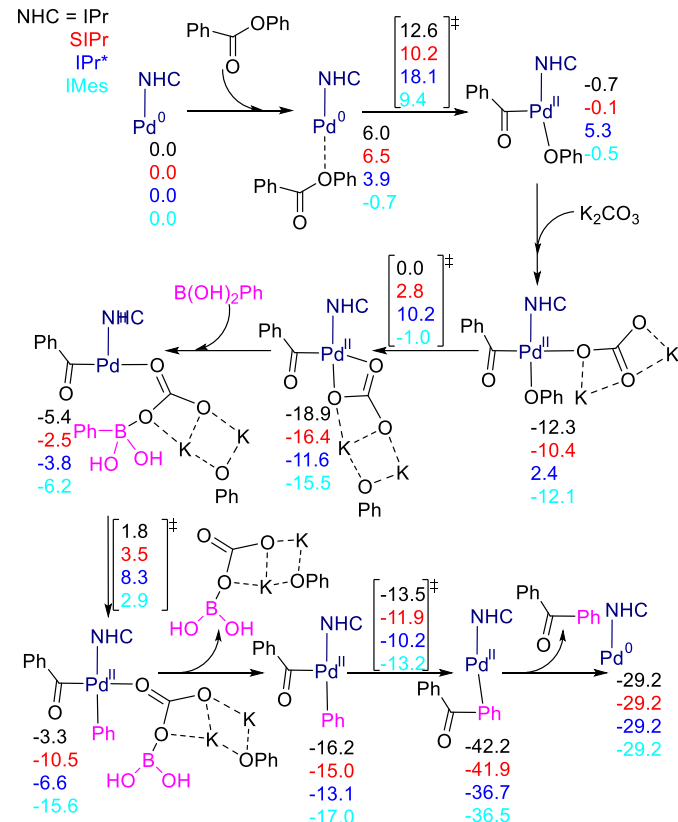


Fig. 4 Optimized Reaction Pathway (relative Energies to Pd(0) in kcal/mol) for the cross-coupling of esters by the catalytic active Pd(NHC) species (in black; NHC = IPr, in red, NHC = SIPr, in dark blue, NHC = IPr*, and in light blue, NHC = IMes).

The extension of the study to other NHC ligands leads to the comparison for the transmetalation since it defines the rate

determining step (rds), with a kinetic cost of 19.9, 15.6 and 21.1 kcal/mol for SIPr, IPr* and IMes; to be compared with the above mentioned 20.7 kcal/mol for IPr. Thus, all those barriers fit perfectly with experimental conditions.

The relatively low energy value for the sterically demanding IPr*,²⁵ and for the sake of consistency, as well, the activation of the dimeric $[\text{Pd}(\text{NHC})(\mu\text{-Cl})\text{Cl}]_2$ precatalysts was checked (see Fig. 5). There, two steps are important in absolute terms, the first involves the dissociative dimer cleavage, with a cost of 17.6, 16.8, 26.6 and 11.9 kcal/mol for IPr, SIPr, IPr* and IMes, respectively. Without commenting on this breakage, the second obstacle corresponds to a double process of transmetalation once a molecule of K_2CO_3 and Ph-B(OH)_2 cooperate to facilitate the phenyl transfer to the metal, with a kinetic cost, the first, of 21.7, 22.1, 23.4 and 23.9 kcal/mol for IPr, SIPr, IPr* and IMes, respectively. And a second costs 23.3, 24.6, 23.6, and 20.5 kcal/mol for IPr, SIPr, IPr* and IMes, respectively. Thus, for IPr* the rds corresponds to the rupture of the initial dimer, while in the other cases it is the transmetalation. But more importantly, catalyst activation is key, as for all catalysts the catalytic cycle is less kinetically expensive.

The nature of the different reagents, focusing only on the phenyl substitution of either aryl addressed in Table 3, was studied computationally, due to significant differences by this simple ring substitution.

Starting from the catalytic rds described the unsubstituted reagents as a reference, the simple insertion of a methyl group in the aryl on boron in para is only worse by 0.9 kcal/mol kinetically speaking. But if this substitution is in ortho, the process gets even worse by 1.3 kcal/mol in agreement with the 75% yield in Table 3. Interestingly, the effect with a simple fluorine confirms the experimental data (98%), with a reduction of the energy barrier of 0.7 kcal/mol; while playing with more intensity with the electronic capacity of the substituents in para, a methoxy group leads to an increase of the energetic barrier of 0.7 kcal/mol; while a substantial reduction of 2.7 kcal/mol with a trifluoromethyl group. This is *a priori* against experiments, but knowing that the activation of the precatalyst is even more kinetically demanding the corresponding rds of the preactivation was calculated to be 23.1, 23.5, 23.8 and 24.0 kcal/mol for the boron based reagent with trifluoromethyl, fluoride, methoxy, methyl and methyl, while for the methyl in ortho this energy cost increases to 28.5 kcal/mol. This latter value agrees perfectly with the experimental 75% yield, as well as all the other values close to 100%, except for trifluoromethyl (81%).

On the other hand, looking at the other reagent, the ester, the differences between substituents located in para show that a methoxy group increases the energy barrier not due to the deterioration of the transition state to be overcome, but to an excessive stabilization of the previous intermediate. Thus, kinetically this energy barrier increases by 1.8 kcal/mol with a methoxy, while it decreases by 1.7, 2.0 and 0.8 kcal/mol, with a methyl, a fluorine, and a trifluoromethyl, respectively. However, with a methyl not in para, but in ortho the cost is much lower, 7.3 kcal/mol. Comparing with the data in Table 3, the borate substituted ring leads to a bad performance for the

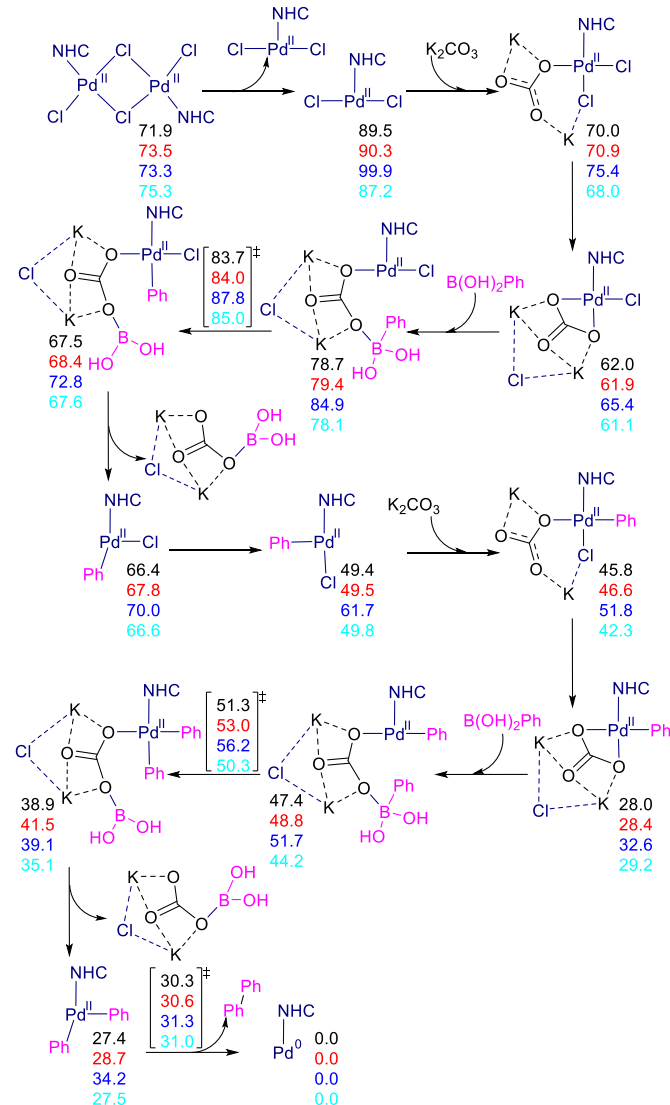


Fig. 5 Optimized Reaction Pathway (relative Energies to $\text{Pd}(0)$ in kcal/mol) for the Activation of Precatalysts $[\text{Pd}(\text{NHC})(\mu\text{-Cl})\text{Cl}]_2$ (in black; NHC = IPr, in red, NHC = SIPr, in dark blue, NHC = IPr*, and in light blue, NHC = IMes).

ortho-methyl substitution, and this might seem in disagreement with calculations. However, for this system the preactivation penalizes the next catalysis, and the overall kinetic cost of 23.3 kcal/mol increases by 5.6 kcal/mol whereas it is maintained for all the other substituents, not in ortho, but in para. All in all, for those, there is a clear trend for the ester substituted ring, with calculations perfectly fitting with the bad results for the methoxy (61%) compared to fluorine (98%). Thus, electronically it is confirmed that this aryl group of the ester prefers an electron-withdrawing group as a substituent on the aryl ring.

Finally, we believe that water facilitates the transmetalation step.^{18a} It is possible that water plays a certain role in the formation and release of the $\text{B(OH)}_2(\text{CO}_3)(\text{OPh})\text{PhK}_2$ unit. Further studies to evaluate if water is able to exchange the carbonate moiety in this and related acyl couplings mediated by Pd–NHC catalyst systems are ongoing.

Conclusions

In summary, we have reported a combined experimental and computational study on the acyl Suzuki–Miyaura cross-coupling of aryl esters mediated by well-defined, air- and moisture-stable Pd(II)–NHC precatalysts $[\text{Pd}(\text{NHC})(\mu\text{-Cl})\text{Cl}]_2$. The following conclusions have been drawn from this study:

(1) $[\text{Pd}(\text{NHC})(\mu\text{-Cl})\text{Cl}]_2$ is the most reactive Pd(II)–NHC precatalyst in the Suzuki–Miyaura cross-coupling of aryl esters by O–C(O) cleavage;

(2) the use of $[\text{Pd}(\text{NHC})(\mu\text{-Cl})\text{Cl}]_2$ leads to broad substrate scope, including late-stage functionalization of pharmaceuticals and chemoselective cross-coupling;

(3) computational studies provide insight into the facile activation of $[\text{Pd}(\text{NHC})(\mu\text{-Cl})\text{Cl}]_2$ to yield the mono-ligated species as the key advantage of this class of Pd(II)–NHC precatalysts versus popular allyl catalysts.

More broadly, the Suzuki–Miyaura cross-coupling of esters using $[\text{Pd}(\text{NHC})(\mu\text{-Cl})\text{Cl}]_2$ proceeds with full selectivity for the C(acyl)–O cleavage to afford versatile ketone products under exceedingly mild conditions. The unique synthetic utility was demonstrated in the direct late-stage functionalization of pharmaceuticals and sequential orthogonal cross-coupling. The reactivity of halo dimer catalysts was found to be in order: Cl > Br > I. The selectivity vs. aryl halides, amides and aliphatic ester bonds has been established. The DFT studies provided insight into the mechanistic details of the catalytic cycle and established the necessary ground for future catalyst and reaction development by selective oxidative addition of the ester C(acyl)–O bond.

This class of Pd(II)–NHC chloro dimer catalysts presents a number of advantages over other classes: (1) robust, scalable one-pot synthesis from NHC salts, (2) commercial-availability, (3) superior atom-economic profile to all other Pd(II)–NHC catalysts, particularly important in light of recent implementation of eco-friendly protocols in cross-coupling, (4) versatile and superb reactivity. Pd(II)–NHC chloro dimer catalysts should be considered as the ‘first-choice’ catalysts for all applications in ester O–C(O) bond activation.

Conflicts of interest

There are no conflicts to declare.

Acknowledgements

We thank Rutgers University, the NSF (CAREER CHE-1650766), and the NIH (1R35GM133326) for generous financial support. Supplement funding for this project was provided by the Rutgers University – Newark Chancellor’s Research Office. The 500 MHz spectrometer used in this study was supported by the NSF-MRI grant (CHE-1229030). A.P. is a Serra Húnter Fellow, and ICREA Academia Prize 2019, and thanks the Spanish MINECO for a project PGC2018-097722-B-I00, and European Fund for Regional Development (FEDER) grant UNGI10-4E-801. S.P.N thanks the BOF research fund as well as the SBO projects CO2perate and D2M for financial support.

Notes and references

- (a) A. de Meijere, S. Bräse and M. Oestreich, *Metal-Catalyzed Cross-Coupling Reactions and More*, Wiley, 2014; (b) G. Molander, J. P. Wolfe and M. Larhed, *Science of Synthesis: Cross-Coupling and Heck-Type Reactions*, Thieme, 2013; (c) T. J. Colacot, *New Trends in Cross-Coupling*, 1st ed., The Royal Society of Chemistry, 2015.
- For perspectives on the historical importance of Pd-catalyzed cross-couplings, see: (a) X. F. Wu, P. Anbarasan, H. Neumann and M. Beller, *Angew. Chem. Int. Ed.*, 2010, **49**, 9047; (b) C. C. C. Johansson-Seechurn, M. O. Kitching, T. J. Colacot and V. Snieckus, *Angew. Chem. Int. Ed.*, 2012, **51**, 5062.
- (a) M. Stradiotto and R. J. Lundgren, *Ligand Design in Metal Chemistry*, Wiley, 2016; (b) M. L. Crawley and B. M. Trost, *Applications of Transition Metal Catalysis in Drug Discovery and Development: An Industrial Perspective*, Wiley, 2012.
- For general reviews on Pd-catalyzed cross-couplings, see: (a) H. Li, C. C. C. Johansson-Seechurn and T. J. Colacot, *ACS Catal.*, 2012, **2**, 1147; (b) P. G. Gildner and T. J. Colacot, *Organometallics*, 2015, **34**, 5497; (c) D. S. Surry and S. L. Buchwald, *Chem. Sci.*, 2011, **2**, 27; (d) P. Ruiz-Castillo and S. L. Buchwald, *Chem. Rev.*, 2016, **116**, 12564. (e) C. Torborg and M. Beller, *Adv. Synth. Catal.*, 2009, **351**, 3027; (f) M. Beller and H. U. Blaser, *Organometallics as Catalysts in the Fine Chemicals Industry*, Springer, 2012; (g) J. Magano and J. R. Dunetz, *Chem. Rev.*, 2011, **111**, 2177; (h) C. A. Busacca, D. R. Fandrick, J. J. Song and C. H. Senanayake, *Adv. Synth. Catal.*, 2011, **353**, 1825; (i) A. Molnar, *Palladium-Catalyzed Coupling Reactions: Practical Aspects and Future Developments*, Wiley, 2013; (j) R. Dorel, C. P. Grugel and A. M. Haydl. *Angew. Chem. Int. Ed.* 2019, **58**, 17118.
- (a) C. M. So and F. Y. Kwong, *Chem. Soc. Rev.*, 2011, **40**, 4963; (b) A. Roglans, A. Pla-Quintana and M. Moreno-Mañas, *Chem. Rev.*, 2006, **106**, 4622; (c) B. M. Rosen, K. W. Quasdorff, D. A. Wilson, N. Zhang, A. M. Resmerita, N. K. Garg and V. Percec, *Chem. Rev.*, 2011, **111**, 1346; (d) J. Cornellà, C. Zarate and R. Martin, *Chem. Soc. Rev.*, 2014, **43**, 8081; (e) M. Tobisu and N. Chatani, *Acc. Chem. Res.*, 2015, **48**, 1717; (f) E. J. Tolleson, L. E. Hanna and E. R. Jarvo, *Acc. Chem. Res.*, 2015, **48**, 2344; (g) Y. F. Zhang and Z. J. Shi, *Acc. Chem. Res.*, 2019, **52**, 161.
- J. F. Hartwig, *Organotransition Metal Chemistry: From Bonding to Catalysis*, University Science Books, 2010.
- For C–O electrophiles, see: (a) T. Zhou and M. Szostak, *Cat. Sci. Technol.*, 2020, **10**, 5702; (b) B. J. Li, D. G. Yu, C. L. Sun and Z. J. Shi, *Chem. Eur. J.*, 2011, **17**, 1728.
- For C–N electrophiles, see: (a) S. B. Blakey and D. W. C. MacMillan, *J. Am. Chem. Soc.*, 2003, **125**, 6046; (b) P. Maity, D. M. Shacklady-McAtee, G. P. A. Yap, E. R. Sirianni and M. P. Watson, *J. Am. Chem. Soc.*, 2013, **135**, 280; (c) J. E. Dander and N. K. Garg, *ACS Catal.*, 2017, **7**, 1413; (d) D. Kaiser, A. Bauer, M. Lemmerer and N. Maulide, *Chem. Soc. Rev.*, 2018, **47**, 7899.
- For C–S electrophiles, see: (a) S. Otsuka, K. Nogi and H. Yorimitsu, *Top. Curr. Chem.*, 2018, **376**, 13; (b) K. Gao, S. Otsuka, A. Baralle, K. Nogi, H. Yorimitsu and A. Osuka, *J. Synth. Org. Chem. Jpn.*, 2016, **74**, 1119; (c) J. Lou, Q. Wang, P. Wu, H. Wang, Y.-G. Zhou and Z. Yu, *Chem. Soc. Rev.*, 2020, **49**, 4307.
- For further recent examples, see: (a) R. M. Yadav, M. Nagaoka, M. Kashihara, R. L. Zhong, T. Miyazaki, S. Sakaki and Y. Nakao, *J. Am. Chem. Soc.*, 2017, **139**, 9423; (b) F. Inoue, M. Kashihara, R. M. Yadav and Y. Nakao, *Angew. Chem. Int. Ed.*, 2017, **56**, 13307; (c) P. Beletskaya, F. Alonso and V. Tyurin, *Coord. Chem. Rev.*, 2019, **385**, 137.
- For reviews on amide cross-coupling, see: (a) S. Shi, S. P. Nolan and M. Szostak, *Acc. Chem. Res.*, 2018, **51**, 2589; (b) G. Meng and M. Szostak, *Eur. J. Org. Chem.*, 2018, **20–21**, 2352; (c) C.

Liu and M. Szostak, *Chem. Eur. J.*, 2017, **23**, 7157; (d) G. Li and M. Szostak, *Chem. Rec.*, 2020, **20**, 649.

12 For reviews on ester cross-coupling, see: (a) R. Takise, K. Muto and J. Yamaguchi, *Chem. Soc. Rev.*, 2017, **46**, 5864; (b) M. Mondal, T. Begum and U. Bora, *Org. Chem. Front.* 2017, **4**, 1430; For the seminal example, see: (c) Y. Yamamoto, J. Ishizu, T. Kohara, S. Komiya and A. Yamamoto, *J. Am. Chem. Soc.*, 1980, **102**, 3758.

13 For reviews on acyl-metals, see: (a) L. J. Gooßen, N. Rodriguez and K. Gooßen, *Angew. Chem. Int. Ed.*, 2008, **47**, 3100; (b) A. Brennführer, H. Neumann and M. Beller, *Angew. Chem. Int. Ed.*, 2009, **48**, 4114.

14 (a) T. B. Halima, W. Zhang, I. Yalaoui, X. Hong, Y. F. Yang, K. N. Houk and S. G. Newman, *J. Am. Chem. Soc.*, 2017, **139**, 1311; (b) P. Lei, G. Meng, S. Shi, Y. Ling, J. An, R. Szostak and M. Szostak, *Chem. Sci.*, 2017, **8**, 6525; (c) S. Shi, P. Lei and M. Szostak, *Organometallics*, 2017, **36**, 3784; (d) A. H. Dardir, P. R. Melvin, R. M. Davis, N. Hazari and M. M. Beromi, *J. Org. Chem.*, 2018, **83**, 469; (e) G. Li, S. Shi, P. Lei and M. Szostak, *Adv. Synth. Catal.*, 2018, **360**, 1538; (f) T. B. Halima, J. K. Vandavasi, M. Shkoor and S. G. Newman, *ACS Catal.*, 2017, **7**, 2176; (g) S. Shi and M. Szostak, *Chem. Commun.* **2017**, **53**, 10584; (h) T. Zhou, G. Li, S. P. Nolan and M. Szostak, *Org. Lett.*, 2019, **21**, 3304; (i) A. A. De la Fuente-Olvera, O. R. Suarez-Castillo and D. Mendoza-Espinosa, *Eur. J. Inorg. Chem.*, 2019, **46**, 4879.

15 For general reviews on Pd-NHCs: (a) S. P. Nolan and C. S. J. Cazin, *Science of Synthesis: N-Heterocyclic Carbenes in Catalytic Organic Synthesis*, Thieme, 2017; (b) S. Diez-Gonzalez, *N-Heterocyclic Carbenes: From Laboratory Curiosities to Efficient Synthetic Tools*, RSC, 2016; (c) S. P. Nolan, *N-Heterocyclic Carbenes*, Wiley, 2014; (d) M. N. Hopkinson, M. N., C. Richter, M. Schedler and F. Glorius, *Nature*, 2014, **510**, 485; (e) C. Valente, S. Calimsiz, K. H. Hoi, D. Mallik, M. Sayah and M. G. Organ, *Angew. Chem. Int. Ed.*, 2012, **51**, 3314; (f) G. C. Fortman and S. P. Nolan, *Chem. Soc. Rev.*, 2011, **40**, 5151; (g) C. S. J. Cazin, *N-Heterocyclic Carbenes in Transition Metal Catalysis*, Springer, 2011; For a review on Pd-NHCs in C–H activations, see: (h) Q. Zhao, G. Meng, S. P. Nolan and M. Szostak, *Chem. Rev.*, 2020, **120**, 1981.

16 T. Zhou, S. Ma, F. Nahra, A. M. C. Obled, A. Poater, L. Cavallo, C. S. J. Cazin, S. P. Nolan and M. Szostak, *iScience*, 2020, **23**, 101377.

17 For pertinent references on Pd–NHC catalysts, see: (a) N. Marion, O. Navarro, J. Mei, E. D. Stevens, N. M. Scott and S. P. Nolan, *J. Am. Chem. Soc.*, 2006, **128**, 4101; (b) O. Navarro, N. Marion, J. Mei and S. P. Nolan, *Chem. Eur. J.*, 2006, **12**, 5142–5148; (c) N. Marion and S. P. Nolan, *Acc. Chem. Res.*, 2008, **41**, 1440; (d) M. S. Viciu, R. M. Kissling, E. D. Stevens and S. P. Nolan, *Org. Lett.*, 2002, **4**, 2229; (e) M. S. Viciu, R. F. Germaneau, O. Navarro-Fernandez, E. D. Stevens and S. P. Nolan, *Organometallics*, 2002, **21**, 5470.

18 For pertinent mechanistic studies, see: (a) G. Li, P. Lei, M. Szostak, E. Casals, A. Poater, L. Cavallo and S. P. Nolan, *ChemCatChem*, 2018, **10**, 3096; (b) G. Magi Meconi, S. V. C. Vummaleti, J. A. Luque-Urrutia, P. Belanzoni, S. P. Nolan, H. Jacobsen, L. Cavallo, M. Solà and A. Poater, *Organometallics*, 2017, **36**, 2088; (c) G. Li, T. Zhou, A. Poater, L. Cavallo, S. P. Nolan and M. Szostak, *Catal. Sci. Technol.*, 2020, **10**, 710; for a DFT study on Ni-catalyzed Suzuki–Miyaura cross-coupling by acyl cleavage, see: (d) C. L. Ji and X. Hong, *J. Am. Chem. Soc.*, 2017, **139**, 15522.

19 U. Christmann and R. Vilar, *Angew. Chem. Int. Ed.*, 2005, **44**, 366.

20 For a review on sterically-demanding NHC ligands, see: F. Izquierdo, S. Manzini and S. P. Nolan, *Chem. Commun.*, 2014, **50**, 14926.

21 D. C. Blakemore, L. Castro, I. Churcher, D. C. Rees, A. W. Thomas, D. M. Wilson and A. Wood, *Nat. Chem.*, 2018, **10**, 383.

22 (a) S. Han, W. Yun, J. Kim, J. Baek, E. Jeong, Y. Kim, Y. Kim, Y. Kim and S. Hwang EP3477722, Oct 31, 2018; (b) S. Y. Hyun and S. U. Jung, KR 2016127428, Apr 27, 2015.

23 G. Meng, S. Shi, R. Lalancette, R. Szostak and M. Szostak, *J. Am. Chem. Soc.*, 2018, **140**, 727.

24 (a) T. Scatolini and S. P. Nolan, *Trends Chem.*, 2020, **2**, 721; (b) J. Sherwood, J. H. Clark, I. J. S. Fairlamb and J. M. Slattery, *Green Chem.*, 2019, **21**, 2164.

25 (a) A. Poater, L. Falivene, C. A. Urbina-Blanco, S. Manzini, S. P. Nolan and L. Cavallo, *Dalton Trans.*, 2013, **42**, 7433; (b) L. Falivene, Z. Cao, A. Petta, L. Serra, A. Poater, R. Oliva, V. Scarano and L. Cavallo, *Nat. Chem.*, 2019, **11**, 872.

Acyl Suzuki–Miyaura Cross-Coupling of Esters: O–C(O) Activation

